*Article*

# Green Synthesis of Gold Nanoparticles for Catalytic Reduction of 4-Nitrophenol and Methylene Blue for Sustainable Development

Muhammad Tahir Khalil [1], Pengxiang Zhang [1], Guosheng Han [1,*], Xianli Wu [1], Baojun Li [1] and Min Xiao [2]

[1] College of Chemistry, Zhengzhou University, Zhengzhou 450001, China; Mtk@gs.zzu.edu.cn (M.T.K.); zhangpxgl@163.com (P.Z.); wuxianli@zzu.edu.cn (X.W.); lbjfcl@zzu.edu.cn (B.L.)

[2] The Key Laboratory of Low-carbon Chemistry & Energy Conservation of Guangdong Province/State Key Laboratory of Optoelectronic Materials and Technologies, School of Materials Science and Engineering, Sun Yat-sen University, Guangzhou 510275, China; stsxm@mail.sysu.edu.cn

* Corresponding author. E-mail: hgs7684@163.com

**ABSTRACT:** Unique structural features and wide applications of gold nanoparticles (GNPs) are inspiring researchers to develop biocompatible, reliable and cost-effective methods for their synthesis. Herein, a clean, eco-friendly and non-toxic method to obtain GNPs was developed by reducing and capping the liquid extract of stem of *Lilium longiflorum* and highlights the catalytic reduction of 4-nitrophenol (4-NP) and methylene blue (MB). The formation of GNPs was confirmed through the absorption peak at 535 nm in the UV-Vis spectra. TEM and HRTEM analyses reveal GNPs spherical morphology with an average size of 4.97 nm. SEM and EDX analyses further elucidate the spherical nature of GNPs and elemental composition. FTIR spectroscopy analysis demonstrates that the GNPs were coated with organic compounds, which prevent the nanoparticle from aggregation. GNPs exhibit remarkable efficiency in reducing 4-NP and MB. The catalytic efficacy of the synthesized GNPs was demonstrated through the enhanced reduction rates of 4-NP and MB, with rate constants of 1.50 min$^{-1}$ and 1.29 min$^{-1}$, respectively. This study develops a novel and eco-friendly technique for the synthesis of gold nanoparticles and opens possibilities for the green synthesis of other metal nanoparticles. The confirmed catalytic activity holds promise for a range of industrial applications and environmental sustainability.

**Keywords:** Gold nanoparticles; Green synthesis; Catalytic reduction; 4-Nitrophenol; Methylene blue

## 1. Introduction

Nanotechnology has revolutionized various fields, including medicine, infrastructure, genomics, and engineering [1]. Gold nanoparticles (GNPs) are particularly intriguing due to unique physicochemical properties, such as size, shape, and surface area [2]. These nanoparticles exhibit a range of optical, biological, catalytic, and sensory properties [3–6], making them ideal for applications in drug delivery, tissue engineering and environmental sensing [7–12]. GNPs can be also used in areas such as sensory and colorimetric probes in therapeutic applications [13], vapour sensing of different organic solvents [14], virus diagnostics [15], pathogen discovery [16], and feature monitoring of food and water [17]. The applications of GNPs largely depend on their sizes. GNPs with size of 100 nm or fewer have abundant novel and extensive applications in microchip technology, chemicals, eco-friendly protection and biological drug [18]. The function in biomedical and other fields will be enhanced with smaller size [19]. The shapes of colloidal GNPs also substantially influence their properties and, consequently, applications [20]. GNPs exhibit various shapes including hexagonal platelets, nano-triangles, hexagonal platelets, nano-prisms, nano-rods and irregular shapes. Amongst all shapes, nanoparticles with triangular shape show more striking optical properties than all others [21].

GNPs can be synthesized via several chemical methods by using NaBH$_4$ [22], sodium citrate [23], or L-ascorbic acid [24] as reducing agents and alkane thiol [25], poly vinyl pyrolidone [26], thiol functionalized imidazolium ionic liquids [27], peptide biphenyl hybrids (PBHs) as stabilizing agents [28]. The development of GNPs through eco-friendly methods has become a crucial field of study, motivated by the demand for sustainability in nanotechnology [29].

Traditional chemical synthesis routes, while effective, often involve toxic reagents and generate hazardous by-products [30]. In contrast, green synthesis approaches utilizing biological entities, such as plant extracts, have gained attention due to their operational simplicity, cost-effectiveness, and minimal ecological impact [31]. This study contributes to green nanotechnology by retaining *Lilium longiflorum* extract, a novel biological agent, for the reduction of gold ions to GNPs. The choice of *Lilium longiflorum* is based on its rich phytochemical profile, numerous phytochemical constituents on the gold nanoparticles surface, including flavonoids, terpenoids, and phenolic acids, which are inherent to the *Lilium longiflorum* extract used [32]. Terpenoids, for instance, contribute hydrophobic interactions that enhance stability [33], while flavonoids and phenolic acids can donate electrons to gold ions, facilitating their reduction and contributing to the capping layer that stabilizes the nanoparticle's surface [34]. These phytochemicals are known for their strong binding affinity to gold, which facilitates the synthesis and stabilization of the nanoparticles. Specifically, the hydroxyl groups in these compounds form a robust capping layer that prevents aggregation by providing steric hindrance and electrostatic stabilization [35]. This bio-coating is critical for maintaining the nanoparticles dispersion stability the reduction of 4-Nitrophenol and methylene blue.

GNPs derived from plant extracts show a wide variety of biological activities, including anti-bacterial, antimicrobial, anticancer, anti-biofouling, anti-malarial, anti-parasitic, antioxidants [36–39] and catalytic activity [40]. GNPs can also be synthesized by green synthetic methods. GNPs can be synthesized by using eggshell membrane (ESM), edible mushroom, biocompatible and biodegradable polymer chitosan, and so on, as accessory reagents.

The utilization of green-synthesized GNPs in catalysis is highly examined, particularly for their catalytic reduction of contaminants, such as p-nitrophenol (4-NP) and methylene blue (MB) [41,42]. These pollutants are residues of the manufacture of herbicides, insecticides, and synthetic fibers, and have been designated as priority pollutants by the US Environmental Protection Agency (EPA) owing to their toxicity. GNPs have shown higher catalytic activity at decreasing the concentrations of these pollutants than typical catalysts [43,44]. And GNPs could be repeatly utilized for many times due to the simplicity of extraction as catalysts. Theerthagiri et al. explored enhancing wastewater treatment by combining photocatalysis with sonolysis, addressing the limitations of traditional methods and the role of advanced materials in pollutant degradation [45]. Naik et al. developed electrochemical sensors utilizing ZnS/Au/f-multi-walled carbon nanotube nanostructures for detect the toxic pollutant 4-nitrophenol (4-NP). The sensor was produced through a sophisticated process to combine pulsed laser-assisted technique and wet chemical methods, demonstrated high sensitivity and selectivity for 4-NP, showing potential for environmental monitoring applications [46]. Theerthagiri et al discussed the electrocatalytic conversion of nitrate waste to ammonia, a process beneficial for both pollution control and ammonia production.[47] Wang et al used Solieria tenuis in a study to make composite materials with gold nanoparticles (Au@PE NPs) that showed excellent abilities for environmental remediation [48]. Deokar and Ingale reported that gold nanoparticles can decrease the toxicity of organic dyes in wastewater, which can lead to better dye removal, decreased pollution, and environment-friendly properties [49].

In this study, the green synthesis of Gold NPs using the liquid extract of *Lilium longiflorum*, a medicinal plant, as reducing, capping and stabling agent. This approach is unique as it utilizes a plant extract widely explored for the synthesis of nanoparticles, offering a sustainable alternative to conventional chemical methods. The green synthesis method ensures biocompatible, reduces the toxicity of the nanoparticles and environmental sustainability. Various factors affecting the stability of these nanoparticles were investigated. However, the prepared gold nanoparticles exhibit high catalytic activity for the reduction of 4-nitrophenol and methylene blue, highlighting their industrial potential. This work will extend the approach to obtain metal NPs in green chemistry and make a contribution for ecological environment optimization.

## 2. Materials and Methods

### 2.1. Materials and Chemical Regents

*Lilium longiflorum* fresh stem was purchased by the market. Gold chloride salt (HAuCl$_4$·3H$_2$O, 99%), Sodium hydroxide (NaOH, ≥99%), Sodium borohydride (NaBH$_4$, ≥99%), Sodium hydrogen carbonate (NaHCO$_3$, ≥99%) were purchased by Shanghai Aladdin Biochemical Technology Co., Ltd. (Shanghai, China). 4-Nitrophenol (C$_6$H$_5$NO$_3$, 99%) and Methylene blue (C$_{16}$H$_{18}$ClN$_3$S, 99%) were purchased by Merck (Darmstadt, Germany). Deionized water (SZ-93A, Shanghai Yarong biochemical instrument factory) was used for all experiments. All chemical reagents were purchased from commercial suppliers and used without further purification.

## 2.2. Characterization Techniques

UV-Visible spectroscopy was recorded on double-beam spectrophotometer (Jasco V-750, Jasco Corporation, Hachioji, Japan) cover a wavelength range from 190 to 800 nm and equipped with 1 cm wide quartz cuvettes. Fourier transform Infrared spectroscopy (FTIR) on KBr pellets was performed on a spectrophotometer (Perkin Elmer, Inc., Waltham, MA, USA). The microstructure of synthesized GNPs was studied on scanning electron microscopy (SEM, ZEISS Sigma 500, ZEISS (Carl Zeiss AG), Oberkochen, Germany) and transmission electron microscopy (TEM, FEI Tecnai $G^2$ F20 S-TWIN electron microscope, Thermo Fisher Scientific (formerly FEI Company), Hillsboro, OR, USA, operated at 200 kV). Samples were prepared for TEM analysis by diluting in methanol a very small volume of GNPs colloid. The mixture was sonicated and one placed onto a carbon coated copper grid and dried. The mean particle size and the size distribution of the produced GNPs were determined using the Nano measurer software (Nano measurer, 1.2, University of Nottingham, Nottingham, UK) by counting more than 100 particles.

## 2.3. Preparation of Aqueous Extract of Stem of Lilium longiflorum

Fresh stem was taken from *Lilium longiflorum* plants and washed with tap water and cut into small pieces for further process. 40 g of fresh small pieces was immersed in 60 mL water and boiled for about 20 minutes. The solid was filtered and the light-yellow filtrate was cooled and used as an aqueous extract for reduction of gold salt.

## 2.4. Synthesis of Gold Nanoparticles

A controlled experiment was carried out for green synthesis of nanoparticles in which 6 mL of plant extract was added to 25 mL solution of $HAuCl_4 \cdot 3H_2O$ (1 mM) at 25 °C. The color of the solution changed from lemon yellow to red ruby (gold ion) indicating the formation of GNPs. The obtained gold nanoparticles were centrifuged (6000 rpm 5 min) and washed with deionize water three times. GNPs were collected after drying in an electric oven (60 °C, 10 h).

## 2.5. Factors Affecting the Synthesis of Gold Nanoparticles

1 mM solution of auric chloride was prepared by dissolving 170 mg of $HAuCl_4 \cdot 3H_2O$ into 500 mL distilled water.

### 2.5.1. Effect of Concentration of Aqueous Extract

6 mL of 1 mM $HAuCl_4 \cdot 3H_2O$ solution was taken into a beaker, and the pH of the solution was neutralized by $NaHCO_3$, and then 0.25 mL liquid extract was added into the beaker. Resulting solution was stirred for 10 mins at room temperature in shady and stayed overnight. Same general procedure was repeated for following concentrations of liquid stem extract: 0.125 mL, 0.5 mL, 1 mL, 1.5 mL, 2 mL. After that UV-Vis spectra of each solution were carried out.

### 2.5.2. Effect of Temperature

6 mL of 1 mM $HAuCl_4 \cdot 3H_2O$ solution was taken into a beaker, and then pH of the solution was neutralized by $NaHCO_3$, and then 0.25 mL liquid extract was added into the beaker. Resulting solution was stirred at room temperature (30 °C) for 10 mins. Same general procedure was repeated for following temperatures: 0 °C, 50 °C, 80 °C and 100 °C. After that UV-Vis spectra of each solution were carried out. Higher temperatures typically increase reaction rates, potentially leading to faster nucleation and growth of nanoparticles. This can result in smaller, more uniform nanoparticles.

### 2.5.3. Effect of Reaction Time

6 mL of 1 mM solution of $HAuCl_4 \cdot 3H_2O$ was taken into a beaker, and the acidity was neutralized by $NaHCO_3$. Then 0.25 mL liquid extract was added into the beaker. Subsequently, solution was heated to 100 °C and kept for 2 mins. After that, UV-Vis spectral study of solution was carried out. Same general procedure was repeated at same temperature and heated it for following time intervals: 4 mins, 6 mins, 8 mins, and 10 mins. Longer reaction times can allow for more growth and possibly aggregation of nanoparticles, affecting their size and distribution.

### 2.5.4. Effect of pH

6 mL solution of 1 mM solution of $HAuCl_4 \cdot 3H_2O$ was taken into a beaker and neutralized by adding $NaHCO_3$, then 0.25 mL of liquid stem extract was added into it. The resulting solution stirred continuously for 10 mins in dark at 100 °C. After that, UV-Vis spectral study of solution was carried out. Same procedure was repeated for following pH of 1, 4, 7, 9 and 12. The pH of auric chloride solution was adjusted by addition of $NaHCO_3$, 1 M NaOH solution and 1 M HCl solution. The pH affects the charge on the gold ions and the extract components, which can alter the rate of reduction and stability of the nanoparticles. Different pH levels lead to variations in particle size and shape.

2.5.5. Effect of Salt

15 mL solution of 1 mM solution of HAuCl$_4$·3H$_2$O taken in a beaker and was neutralized by adding NaHCO$_3$. Then 1 mL of liquid stem extract was added into it. The resulting solution was stirred continuously for 10 min and divided into 5 equal parts in five flasks. 2 mL of 1 M, 2 M, 3 M, 4 M and 5 M solution was added in each flask, respectively and changing salt concentration impacts the ionic strength and electrostatic interactions in the solution, which can influence nanoparticle aggregation and stability. After 24 h, UV-Vis spectral analysis of each solution was performed.

To check stability of gold nanoparticles formed, UV-Vis spectra of reaction mixture were taken for each 24 h until 20–25 days.

## 2.6. Catalytic Performance Evaluation of GNPs

### 2.6.1. Catalytic Reduction of 4-NP by GNPs

The standard reduction of 4-NP by NaBH4 is as following: 1 mL of 2 mM solution of 4-NP, 1 mL of 0.02 M NaBH4 and 1 mL distilled water taken in cuvette and take first reading instantly by UV-Vis spectrophotometer at 400 nm then after 5 mins in regular intervals till complete reduction occur. Then 1 mL of 2 mM solution of 4-NP, 1 mL of 0.02 M NaBH4, 1 mL distilled water and 0.2 mL of highly saturated solution of GNPs (1 mg) were taken into cuvette and take reading in regular intervals. 0.1 mL (0.5 mg), 0.05 mL (0.25 mg) and 0.01 mL (0.05 mg) GNPs were added as a condition for investigation and checked in regular intervals till completion of reduction.

### 2.6.2. Catalytic reduction of MB by GNPs

The promising application of GNPs is the catalytic reduction of liquid MB to leuco-MB by NaBH4. The standard reduction of MB by NaBH4 is as following: 1 mL of 10 ppm solution of MB, 1 mL of 0.02 M NaBH4, 1 mL distilled water were taken into cuvette and the reaction was instantly checked by UV spectrophotometer at 665 nm, and then after 5 mins in regular intervals till completion of the reaction. 1 mL of 10 ppm solution of methylene blue, 1 mL of 0.02 M NaBH4, 1mL distilled water and 0.2 mL (1 mg) of highly saturated solution of GNPs were taken into cuvette and checked the absorbance at 665 nm in regular interval as above. 0.1 mL (0.5 mg), 0.05 mL (0.25 mg) and 0.01 mL (0.05 mg) GNPs were added as a condition for investigation and checked in regular intervals till completion of reduction.

## 3. Results and Discussion

### 3.1. Preparation and Characterization of GNPs

Aqueous gold solution is light yellow in color (Figure 1a) and color of liquid extract of *Lilium longiflorum* stem is lemon yellow (Figure 1b). Color of gold solution remains unchanged as addition of liquid extract at first. When the mixed solution was kept overnight, the color changed into ruby red (Figure 1c). A peak at 535 nm appeared in its UV-Vis spectra (Figure 2a), which specified the formation of gold nanoparticles [50–52].
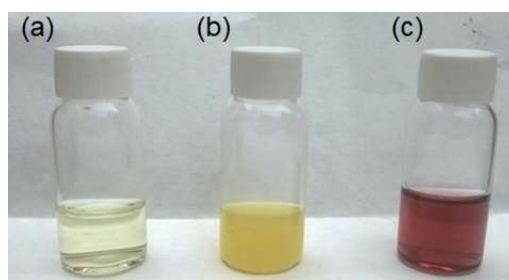


**Figure 1.** (**a**) HAuCl$_4$·3H$_2$O solution (**b**) Liquid extract of *Lilium longiflorum* stem (**c**) GNPs solution.

An important factor affecting synthesis of GNPs is quantity of liquid extract. An extensive range of fluctuating volumes, 0.125 mL, 0.25 mL, 0.50 mL, 1.0 mL, 1.5 mL and 2.0 mL of liquid extract, were added into 6 mL of 1 mM solution of HAuCl$_4$·3H$_2$O at room temperature in neutral medium, respectively. The UV-Vis spectra (Figure 2b) show that the optimal volume ratio for synthesis of GNPs is 0.25 mL with 6 mL of 1 mM solution of HAuCl$_4$·3H$_2$O. As liquid extract was used, the color was light pink and when the quantity of liquid is 0.125, 0.50, 1.0 mL or more, there is no sharp ruby red color appeared and the peak at 535 nm was not obvious.

To explore the optimal reaction temperature, different temperatures, 0, 30, 50, 80, 100 °C, were adopted at neutral medium. The UV-Vis spectra (Figure 2c) indicate a steady rise in absorbance at 535 nm with increase of temperature. A sharp ruby red color is obtained at 100 °C for 10 mins heating. Maximum absorption was observed by heating at 100 °C.

Reaction time is also important factor affecting synthesis of GNPs. Reactions were carried out at neutral pH and 100 °C for 2, 4, 6, 8 and 10 mins. The UV-Vis spectra (Figure 2d) of each solution show that maximum absorbance was achieved by heating reaction for 8minutes and 10 mins and very fine peaks were observed. However, no color change and absorption peak were observed by heating for 2 and 4 mins. After 6 mins, slight change in color was observed and there is an absorption peak at 535 nm. However, by 30 mins heating, broad peak appears due to formation of purple color particles.

Green synthesis of GNPs was carried out under wide pH range of 1, 3, 7, 9, and 11. Basic and acidic conditions are not favorable for synthesis of GNPs. At pH 1, no color change was observed. At pH 4, color changes to blue shade and at basic pH color changes to purple black. UV-Vis spectra (Figure 2e) verified that neutral environments are best for green synthesis of GNPs. Maximum absorbance achieved at neutral pH.

To study the stability of GNPs to salt effect, reaction mixtures were preserved with variable concentrations of NaCl, including 1, 2, 3, 4 and 5 M. The UV-Vis spectra (Figure 2f) illustrate that salt effect can greatly influence the stability of GNPs, which results in decomposition of gold nanoparticles and leads to aggregation in salt solution. Stability of GNPs under optimal conditions was detected above period of 20–25 days. The UV-Vis spectra (Figure 2g) illustrated that the stability of biosynthesize GNPs can be kept for more than 17 days. After that gold nanoparticles start to coagulate.

The Fourier Transform Infrared (FTIR) spectroscopy analysis provides compelling insights into the structure of compound. The FTIR spectra (Figure 2h) of GNPs obtained a 3437 cm$^{-1}$ and 3711 cm$^{-1}$ are characteristic of hydroxyl groups, indicative of polyphenols, which are active in the reduction of gold ions to nanoparticles. The peak at 2915 cm$^{-1}$ identifies aliphatic hydrocarbon chains, typically from fatty acids. The sharp peak at 1761 cm$^{-1}$ is attributed to carbonyl groups, representing esters and carboxylic acids, which commonly cap and stabilize nanoparticles. The peak at 1523 cm$^{-1}$ denotes aromatic ring structures, a characteristic of polyphenolic compounds that provide antioxidant properties. The peak at 1037 cm$^{-1}$ aligns with C–O stretching vibrations found in plant-derived ethers and alcohols. The peak at 882 cm$^{-1}$ corresponds to C–H bending in trans-alkenes, signaling unsaturated compounds, while the peak at 557 cm$^{-1}$ is associated with metal-oxygen bonds, indicative of the interaction between gold ions and oxygen-containing functional groups, essential for nanoparticle formation and stabilization. These functional groups delineate a phytochemical profile within the plant extract that directly contributes to the formation and stabilization of gold nanoparticles. It is evident from the analysis bands are linked with the polyphenol group. The comparison of the FTIR spectra of GNPs revealed that the absorption bands of the hydroxyl, carbonyl, and aromatic rings groups shifted. This collective data clearly show GNPs were coated by a layer of organic compounds from the stem extract, which prevent the aggregation of nanoparticles.
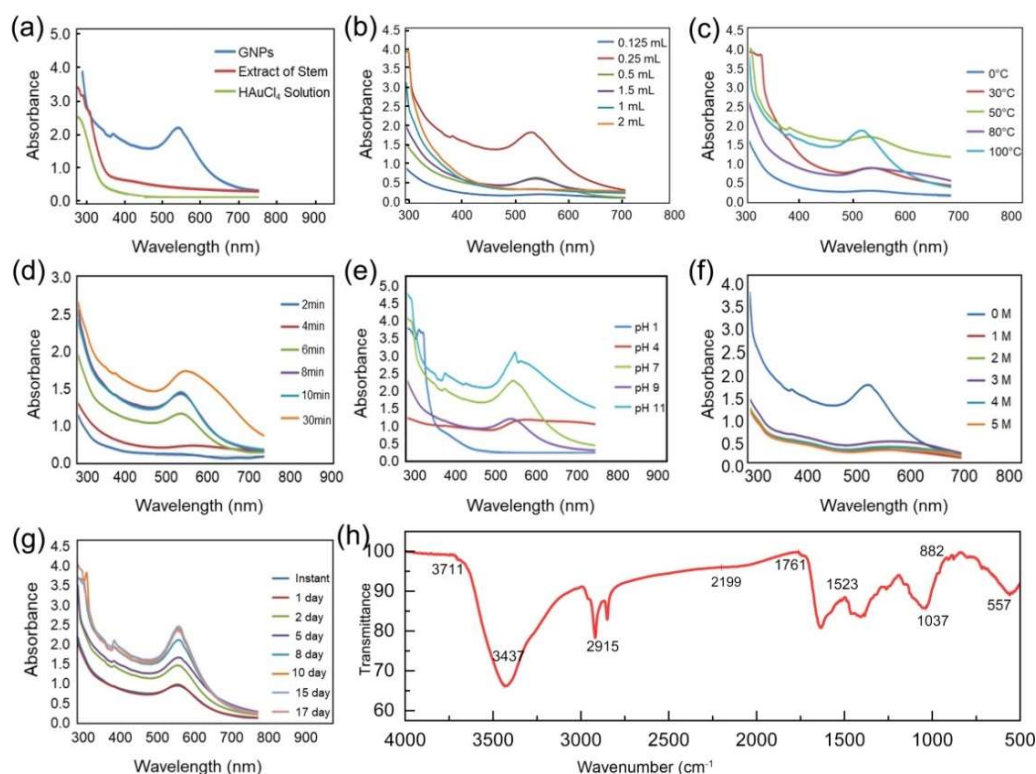


**Figure 2.** (**a**) UV-Vis spectra of liquid extract of stem of *Lilium longiflorum,* GNPs, and HAuCl$_4$ solution. The UV-Vis spectra of GNPs gotten at different conditions: (**b**) different volumes of extract (**c**) different temperatures, (**d**) different reaction time, (**e**) different acidity. (**f**) different salt concentration, (**g**) kept for different time. (**h**) FTIR spectroscopy of GNPs obtained at optimum conditions.

TEM images reveal the formation of GNPs obtained under optimal conditions (Figures 3a and 3b). The mean size of GNPs appears to be 4.97 nm (inset of Figure 3b). The high resolution (HRTEM) images express the high crystallinity with interfacial interaction and d-spacing of 0.12 nm [53] in (Figure 3c). Scanning transmission electron microscopic high angle-annular dark field (STEM-HAADF) images show the existence and uniform distribution of Au, C, Na and O elements in (Figure 3d) and elemental mapping images with atomic compositions of 1.90%, 92.15%, 0.49%, and 5.44%, respectively (Inset of Figure 3e). The scanning electron microscope (SEM) images indicate the spherical morphology of GNPs (Figure 3e–f). Thus, these results ensure the successful preparation of GNPs.
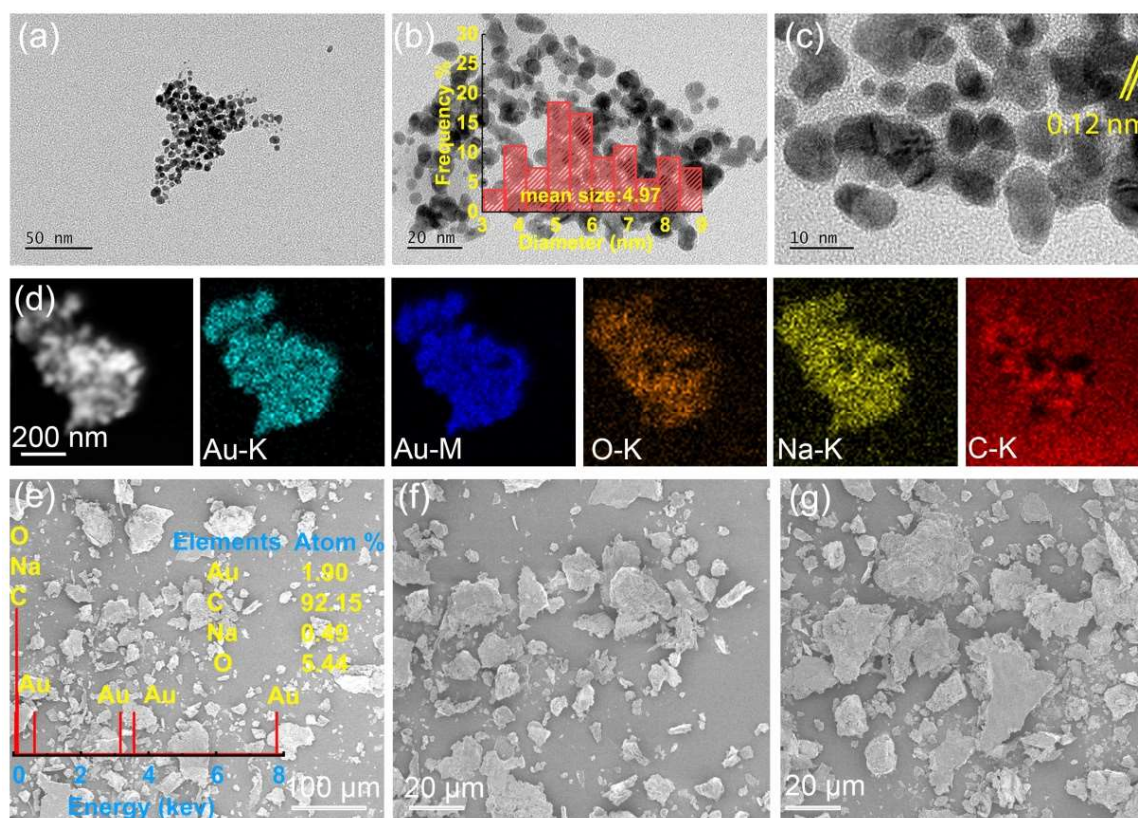


**Figure 3.** (**a**) TEM image, (**b**) TEM image with inset histogram of GNPs size, (**c**) High-resolution TEM image (HRTEM) image, (**d**) STEM-HAADF and elemental mapping images of GNPs, (**e**) Scanning electron microscope images with inset of EDX spectrum, (**f, g**) SEM micrographs.
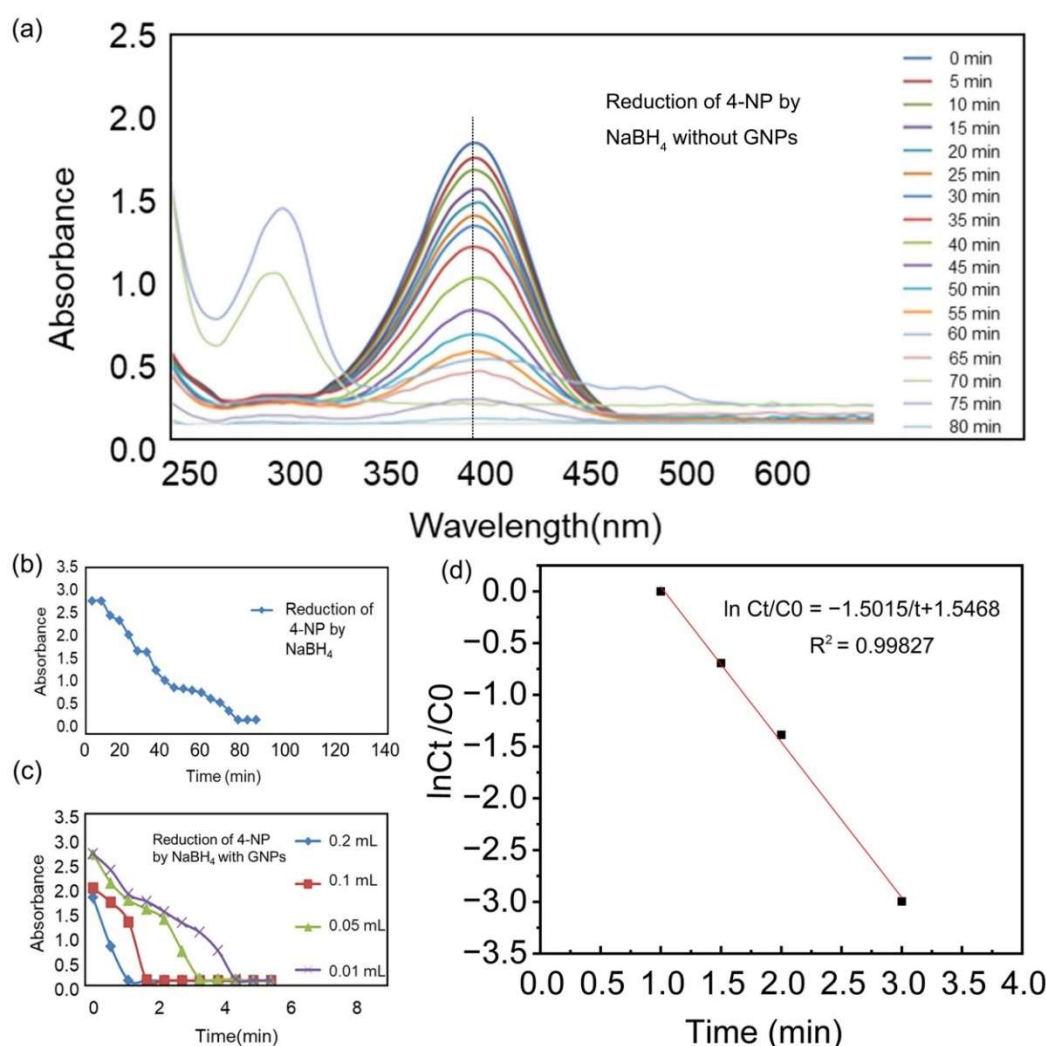
## 3.2. Catalytic Activity Evaluation of GNPs

### 3.2.1. Catalytic Reduction of 4-NP

UV-Vis analysis was used to determine reduction in liquid medium. The absorption peak of 4-NP is at 400 nm. About 80 mins were needed to finish the reduction reaction without GNPs (Figure 4a). The difference of reaction time between reduction of 4-NP by NaBH4 with and without GNPs was studied. And the reduction of 4-NP by NaBH$_4$ without GNPs in (Figure 4b). While the reduction time drops down to several minutes when GDPs were introduced as catalyst in very small amount (Figure 4c). By using 0.2 mL (1 mg) in 1 min and 0.1 mL (0.5 mg) GNPs, reduction reaction finished in 1.5 min. And by using 0.05 mL (0.25 mg) and 0.01 mL (0.05 mg) GNPs as catalyst, the reaction time reduces to 2 and 3 mins. GNPs significantly improved the reduction rate of 4-nitrophenol. Specifically, the reduction process was notably more rapid when using a higher concentration of GNPs. The kinetics of the reduction of 4-NP with pseudo-first order law:

$$\ln(C_t/C_0) = -k_{app}t \tag{1}$$

where $C_t$ is the concentration of solution at different times, $k_{app}$ is the apparent rate constant and $t$ is the reaction time (min). The value of $k_{app}$ was obtained from the slope of the graph of $\ln(C_t/C_0)$ vs. time (Figure 4d) The rate constants have been determined 1.50 min$^{-1}$ and R square is 0.99827. Previous studies showed that in general, the rate of the reduction reaction depends on the size of the NPs because smaller particles stimulate the adsorption of reagents on their surface [53,54].

**Figure 4.** (**a**) The UV-Vis spectra of 4-NP in different time in liquid medium without catalyst. (**b**) The reaction time of 4-NP reduced by NaBH₄ without GNPs. (**c**) The reaction time of 4-NP reduced by NaBH₄ with GNPs as catalyst. (**d**) First-Order Reaction Kinetics for the reduction of 4-NP by NaBH₄ in the presence of GNPs.
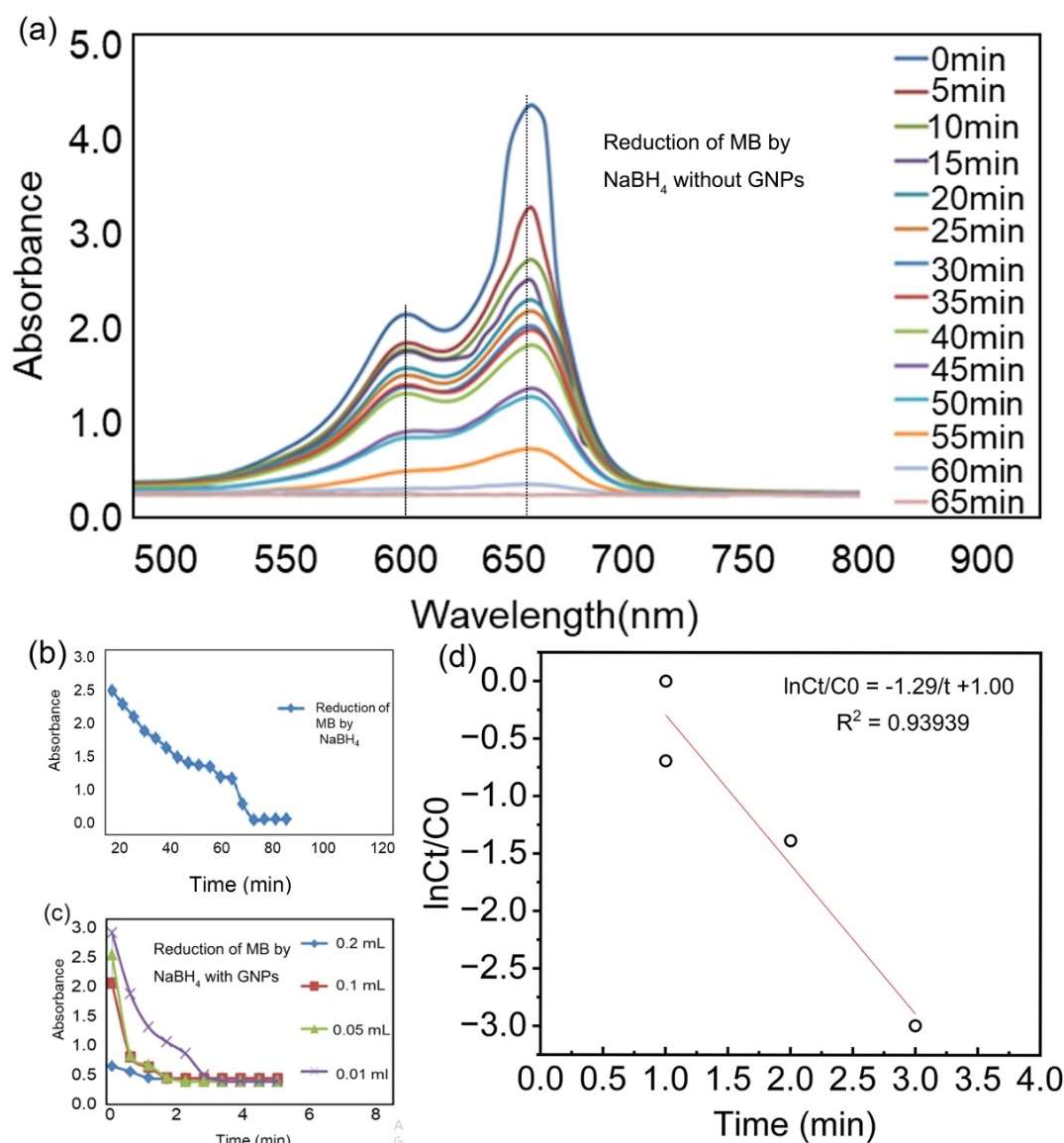
### 3.2.2. Catalytic Reduction of MB

UV-Vis analysis was used to determine reduction in liquid medium. Absorption peaks of MB are at 665 and 614 nm. The UV-Vis spectra show that the reduction reaction needs 65 min to finish by NaBH4 without GNPs as catalyst (Figure 5a,b). The reduction process was greatly accelerated with GNPs as catalyst. The reduction reaction finished in 2–3 min (Figure 5c). The time required for a complete reduction has been modified based on the concentration of the GNPs. Primarily when a high concentration of GNPs is used the reaction time decreased. 0.2 mL (equal to 1 mg) of GNPs is used, and the reduction is completed in 1 min. A slightly lower concentration of 0.1 mL (0.5 mg) gave the same fast result as the one-minute completion time. As a minimum concentration of 0.05 mL (0.25 mg) was used, 2 mins were needed. Furthermore, the total reduction took three minutes when the concentration of GNPs was reduced to 0.01 mL (0.05 mg). These observations show that the total reaction time is reversed to the GNP concentration used. Higher concentrations show shorter reduction time, and lower concentrations require longer. In the reaction process, MB is electrophilic toward GNPs in environment. GNPs take electrons from BH4- ion and transfer them to MB. The kinetics of the reduction of MB with pseudo-first order law:

$$\ln(C_t/C_0) = -k_{app}t \qquad (2)$$

where $C_t$ is the concentration of solution at different times, $k_{app}$ is the apparent rate constant and $t$ is the reaction time (min). The value of $k_{app}$ was obtained from the slope of the graph of $\ln(C_t/C_0)$ vs. time (Figure 5d) The rate constants have been determined 1.29 min$^{-1}$ and R$^2$ 0.93939. Results indicate that rate of reduction increases in the presence of GNPs as a catalyst.

Previous studies have shown that the catalytic performance of green synthesized NPs depends on their size and shape. Smaller GNPs led to faster reduction due to increased surface area and ion adsorption [55–57].

**Figure 5:** (**a**) The UV-Vis spectra of MB in different time in liquid medium without catalyst. (**b**) The reaction time of MB reduced by NaBH$_4$ without GNPs. (**c**) The reaction time of MB reduced by NaBH$_4$ with GNPs as catalyst. (**d**) Reaction Kinetics for the reduction of MB by NaBH$_4$ in the presence of GNPs.

## 4. Conclusions

This study effectively addresses an eco-friendly, efficient, and reliable method for synthesizing gold nanoparticles. Utilizing the liquid extract from the stem of *Lilium longiflorum* as raw materials, we achieved the green synthesis of gold nanoparticles and ensured their stability and functionality. UV-Vis spectroscopy was confirmed GNP formation with absorption peak at 535 nm. TEM and SEM studies show GNPs uniform spherical shape and an average size of 4.97 nm. FTIR results show that organic compounds from the extract stabilize the GNPs and prevent aggregation. The GNPs demonstrate excellent catalytic efficiency in the reduction of 4-NP and MB through kinetic studies, revealing rate constants of 1.50 min$^{-1}$ and 1.29 min$^{-1}$, respectively. This highlights the potential of GNPs in environmental remediation, size and concentration play critical roles in their catalytic performance. These findings have significant industrial and environmental implications, particularly regarding waste treatment and environmental remediation. This research offers a sustainable alternative to conventional chemical nanoparticle synthesis methods, thereby contributing to the broader goals of green chemistry and sustainable nanotechnology. The study also makes new promises for applying this green synthesis approach to other metal nanoparticles.

## Acknowledgments

## Author Contributions

Writing—Original Draft Preparation, Investigation, Data Curation: M.T.K.; Methodology, Formal Analysis, Visualization: P.Z.; Conceptualization, Supervision, Writing—Review & Editing: G.H.; Writing—Review & Editing, Funding Acquisition, Project Administration: X.W.; Writing—Review & Editing, Formal Analysis: B.L. and M.X.

## Declaration of Competing Interest

The authors declare no competing interest.

## References

1. Ahmad N, Bhatnagar S, Saxena R, Iqbal D, Ghosh A, Dutta R. Biosynthesis and characterization of gold nanoparticles: Kinetics, in vitro and in vivo study. *Mater. Sci. Eng. C* **2017**, *78*, 553–564.
2. Ahmad T, Bustam MA, Irfan M, Moniruzzaman M, Asghar HMA, Bhattacharjee S. Green synthesis of stabilized spherical shaped gold nanoparticles using novel aqueous *Elaeis guineensis* (oil palm) leaves extract. *J. Mol. Struct.* **2018**, *1159*, 167–173.
3. Ahmad T, Bustam MA, Irfan M, Moniruzzaman M, Asghar HMA, Bhattacharjee S. Mechanistic investigation of phytochemicals involved in green synthesis of gold nanoparticles using aqueous *Elaeis guineensis* leaves extract: Role of phenolic compounds and flavonoids. *Biotechnol. Appl. Biochem.* **2019**, *66*, 698–708.
4. Aldewachi H, Chalati T, Woodroofe M, Bricklebank N, Sharrack B, Gardiner P. Gold nanoparticle-based colorimetric biosensors. *Nanoscale* **2018**, *10*, 18–33.
5. Alegria EC, Ribeiro AP, Mendes M, Ferraria AM, Rego AMBd, Pombeiro AJ. Effect of phenolic compounds on the synthesis of gold nanoparticles and its catalytic activity in the reduction of nitro compounds. *Nanomaterials* **2018**, *8*, 320.
6. Amendola V, Pilot R, Frasconi M, Maragò OM, Iatì MA. Surface plasmon resonance in gold nanoparticles: A review. *J. Phys. Condens. Matter* **2017**, *29*, 203002.
7. Azubel M, Kornberg RD. Synthesis of water-soluble, thiolate-protected gold nanoparticles uniform in size. *Nano Lett.* **2016**, *16*, 3348–3351.
8. Bahrulolum H, Nooraei S, Javanshir N, Tarrahimofrad H, Mirbagheri VS, Easton AJ, et al. Green synthesis of metal nanoparticles using microorganisms and their application in the agrifood sector. *J. Nanobiotechnol.* **2021**, *19*, 1–26.
9. Balciunaitiene A, Viskelis P, Viskelis J, Streimikyte P, Liaudanskas M, Bartkiene E, et al. Green Synthesis of Silver Nanoparticles Using Extract of *Artemisia absinthium* L., *Humulus lupulus* L. and *Thymus vulgaris* L., Physico-Chemical Characterization, Antimicrobial and Antioxidant Activity. *Processes* **2021**, *9*, 1304.
10. Bansal K, Aqdas M, Kumar M, Bala R, Singh S, Agrewala JN, et al. A facile approach for synthesis and intracellular delivery of size tunable cationic peptide functionalized gold nanohybrids in cancer cells. *Bioconjug. Chem.* **2018**, *29*, 1102–1110.
11. Besenhard MO, Baber R, LaGrow AP, Mazzei L, Thanh NT, Gavriilidis A. New insight into the effect of mass transfer on the synthesis of silver and gold nanoparticles. *Cryst. Eng. Comm.* **2018**, *20*, 7082–7093.
12. Botteon CEA, Silva LB, Ccana-Ccapatinta GV, Silva TS, Ambrosio SR, Veneziani RCS, et al. Biosynthesis and characterization of gold nanoparticles using Brazilian red propolis and evaluation of its antimicrobial and anticancer activities. *Sci. Rep.* **2021**, *11*, 1974.
13. Capek I. Polymer decorated gold nanoparticles in nanomedicine conjugates. *Adv. Colloid Interface Sci.* **2017**, *249*, 386–399.
14. Fromme T, Tintrop LK, Reichenberger S, Schmidt TC, Barcikowski S. Impact of Chemical and Physical Properties of Organic Solvents on the Gas and Hydrogen Formation during Laser Synthesis of Gold Nanoparticles. *Chem. Phys. Chem.* **2023**, *24*, e202300089.
15. Prakashan D, Shrikrishna NS, Byakodi M, Nagamani K, Gandhi S. Gold nanoparticle conjugate-based lateral flow immunoassay (LFIA) for rapid detection of RBD antigen of SARS-CoV-2 in clinical samples using a smartphone-based application. *J. Med. Virol.* **2023**, *95*, e28416.
16. Kang MG, Khan F, Tabassum N, Cho KJ, Jo DM, Kim YM. Inhibition of Biofilm and Virulence Properties of Pathogenic Bacteria by Silver and Gold Nanoparticles Synthesized from *Lactiplantibacillus* sp. Strain C1. *ACS Omega* **2023**, *8*, 9873–9888.
17. Liu H, Baghayeri M, Amiri A, Karimabadi F, Nodehi M, Fayazi M, et al. A strategy for As (III) determination based on ultrafine gold nanoparticles decorated on magnetic graphene oxide. *Environ. Res.* **2023**, *231*, 116177.
18. Hossain N, Mobarak MH, Mimona MA, Islam MA, Hossain A, Zohur FT, et al. Advances and significances of nanoparticles in semiconductor applications-A review. *Results Eng.* **2023**, *19*, 101347.
19. Sanchis-Gual R, Coronado-Puchau M, Mallah T, Coronado E. Hybrid nanostructures based on gold nanoparticles and functional coordination polymers: Chemistry, physics and applications in biomedicine, catalysis and magnetism. *Coord. Chem. Rev.* **2023**, *480*, 215025.
20. Vinnacombe-Willson GA, Conti Y, Stefancu A, Weiss PS, Cortes E, Scarabelli L. Direct Bottom-Up in Situ Growth: A Paradigm Shift for Studies in Wet-Chemical Synthesis of Gold Nanoparticles. *Chem. Rev.* **2023**, *123*, 8488–8529.

21. Kumari M, Pandey S, Giri VP, Nautiyal CS, Mishra A. A critical review on green approaches in shape and size evolution of metal nanoparticles and their environmental applications. *Environ. Nanotechnol. Monit. Manag.* **2023**, *20*, 100895.

22. Ali MY, Abdulrahman HB, Ting WT, Howlader MM. Green synthesized gold nanoparticles and CuO-based nonenzymatic sensor for saliva glucose monitoring. *RSC Adv.* **2024**, *14*, 577–588.

23. Dickson J, Weaver B, Vivekanand P, Basu S. Anti-neoplastic Effects of Gold Nanoparticles Synthesized Using Green Sources on Cervical and Melanoma Cancer Cell Lines. *BioNanoSci* **2023**, *13*, 194–202.

24. Hosny M, Fawzy M, Abdelfatah AM, Fawzy EE, Eltaweil AS. Comparative study on the potentialities of two halophytic species in the green synthesis of gold nanoparticles and their anticancer, antioxidant, and catalytic efficiencies. Adv. *Powder Technol.* **2021**, *32*, 3220–3233.

25. Borsley S, Edwards W, Mati IK, Poss G, Diez-Castellnou M, Marro N, et al. A general one-step synthesis of alkanethiyl-stabilized gold nanoparticles with control over core size and monolayer functionality. *Chem. Mater.* **2023**, *35*, 6168–6177.

26. Huang X, Devi S, Bordiga M, Brennan CS, Xu B. Phenolic compounds-mediated biosynthesis of gold nanoparticles and evaluation of their bioactivities: A review. *Int. J. Food Sci. Technol.* **2023**, *58*, 1673–1694.

27. Kaymaz SV, Nobar HM, Sarıgul H, Soylukan C, Akyuz L, Yuce M. Nanomaterial surface modification toolkit: Principles, components, recipes, and applications. *Adv. Colloid Interface Sci.* **2023**, *322*, 103035.

28. Abbas M, Susapto H, Hauser C. Synthesis and Organization of Gold-Peptide Nanoparticles for Catalytic Activities. *ACS Omega* **2022**, *7*, 2082–2090.

29. Ahmed SF, Mofijur M, Rafa N, Chowdhury AT, Chowdhury S, Nahrin M, et al. Green approaches in synthesising nanomaterials for environmental nanobioremediation: Technological advancements, applications, benefits and challenges. *Environ. Res.* **2022**, *204*, 111967.

30. Gupta D, Thakur A, Gupta TK. Green and sustainable synthesis of nanomaterials: Recent advancements and limitations. *Environ. Res.* **2023**, *231*, 116316.

31. Sabeena G, Rajaduraipandian S, Pushpalakshmi E, Alhadlaq HA, Mohan R, Annadurai G, et al. Green and chemical synthesis of CuO nanoparticles: A comparative study for several in vitro bioactivities and in vivo toxicity in zebrafish embryos. *J. King Saud Univ. Sci.* **2022**, *34*, 102092.

32. Chinnasamy R, Chinnaperumal K, Venkatesan M, Jogikalmat K, Cherian T, Willie P, Malafaia G. Eco-friendly synthesis of Ag-NPs using *Endostemon viscosus* (Lamiaceae): Antibacterial, antioxidant, larvicidal, photocatalytic dye degradation activity and toxicity in zebrafish embryos. *Environ. Res.* **2023**, *218*, 114946.

33. Al-Hayanni H, Alnuaimi M, AL-Lami R, Zaboon S. Antibacterial Effect of Silver Nanoparticles Prepared from Sophora flavescens Root Aqueous Extracts against Multidrug-resistance *Pseudomonas aeruginosa* and *Staphylococcus aureus*. *J. Pure Appl. Microbiol.* **2022**, *16*, 2880–2890.

34. Kumar S, Korra T, Thakur R, Arutselvan R, Kashyap AS, Nehela Y, Keswani C. Role of Plant Secondary Metabolites in Defence and Transcriptional Regulation in Response to Biotic Stress. *Plant Stress* **2023**, *8*, 100154.

35. Bhati M. Biogenic synthesis of metallic nanoparticles: Principles and applications. *Mater. Today Proc.* **2021**, *81*, 882–887.

36. Porras G, Chassagne F, Lyles J, Marquez L, Dettweiler M, Salam A, et al. Ethnobotany and the Role of Plant Natural Products in Antibiotic Drug Discovery. *Chem. Rev.* **2020**, *121*, 3495–3560.

37. Kumari MM, Jacob J, Philip D. Green synthesis and applications of Au–Ag bimetallic nanoparticles. *Spectrochim. Acta Part A Mol. Biomol. Spectrosc.* **2015**, *137*, 185–192.

38. Kureshi AA, Vaghela HM, Kumar S, Singh R, Kumari P. Green synthesis of gold nanoparticles mediated by Garcinia fruits and their biological applications. *Pharm. Sci.* **2020**, *27*, 238–250.

39. Lee KX, Shameli K, Yew YP, Teow SY, Jahangirian H, Rafiee-Moghaddam R, Webster TJ. Recent developments in the facile bio-synthesis of gold nanoparticles (AuNPs) and their biomedical applications. *Int. J. Nanomed.* **2020**, *15*, 275–300.

40. Lunin AV, Korenkov ES, Mochalova EN, Nikitin MP. Green synthesis of size-controlled in vivo biocompatible immunoglobulin-based nanoparticles by a swift thermal formation. *ACS Sustain. Chem. Eng.* **2021**, *9*, 13128–13134.

41. Choudhary BC, Paul D, Gupta T, Tetgure SR, Garole VJ, Borse AU, Garole DJ. Photocatalytic reduction of organic pollutant under visible light by green route synthesized gold nanoparticles. *J. Environ. Sci.* **2017**, *55*, 236–246.

42. Manosalva N, Tortella G, Cristina Diez M, Schalchli H, Seabra AB, Durán N, et al. Green synthesis of silver nanoparticles: Effect of synthesis reaction parameters on antimicrobial activity. *World J. Microbiol. Biotechnol.* **2019**, *35*, 1–9.

43. Mu F, Miao X, Cao J, Zhao W, Yang G, Zeng H, et al. Integration of plasmonic effect and S-scheme heterojunction into gold decorated carbon nitride/cuprous oxide catalyst for photocatalysis. *J. Clean. Prod.* **2022**, *360*, 131948.

44. Agnihotri P, Dan A. Temperature-and pH-Responsive Hydrogel Nanoparticles with Embedded Au Nanoparticles as Catalysts for the Reduction of Dyes. *ACS Appl. Nano Mater.* **2022**, *5*, 10504–10515.

45. Theerthagiri J, Lee SJ, Karuppasamy K, Arulmani S, Veeralakshmi S, Ashokkumar M, et al. Application of advanced materials in sonophotocatalytic processes for the remediation of environmental pollutants. *J. Hazard. Mater.* **2021**, *412*, 125245.

46. Naik SS, Lee SJ, Theerthagiri J, Yu Y, Choi MY. Rapid and highly selective electrochemical sensor based on ZnS/Au-decorated f-multi-walled carbon nanotube nanocomposites. *J. Hazard. Mater.* **2021**, *418*, 126269.

47. Theerthagiri J, Park J, Das HT, Rahamathulla N, Cardoso ES, Murthy AP, et al. Electrocatalytic conversion of nitrate waste into ammonia: A review. *Environ. Chem. Lett.* **2022**, *20*, 2929–2949.

48. Wang L, Qiang X, Song Y, Wang X, Gu W, Niu J, et al. Green synthesis of gold nanoparticles by phycoerythrin extracted from Solieria tenuis as an efficient catalyst for 4-nitrophenol reduction and degradation of dyes in wastewater. *Mater. Today Sustain.* **2023**, *23*, 100435.

49. Deokar GK, Ingale AG. Exploring effective catalytic degradation of organic pollutant dyes using environment benign, green engineered gold nanoparticles. *Inorg. Chem. Commun.* **2023**, *151*, 110649.

50. Garg N, Rastogi L, Bera S, Ballal A, Balramkrishna M. ArsenazoIII functionalized gold nanoparticles: SPR based optical sensor for determination of uranyl ions (UO22+) in groundwater. *Green Anal. Chem.* **2022**, *3*, 100032.

51. Kadu P, Gadhe L, Navalkar A, Patel K, Kumar R, Sastry M, et al. Charge and hydrophobicity of amyloidogenic protein/peptide templates regulate the growth and morphology of gold nanoparticles. *Nanoscale* **2022**, *14*, 15021–15033.

52. Kaur K, Ahmed B, Singh J, Rawat M, Kaur G, Al Kahtani M, et al. *Bryonia laciniosa Linn* mediated green synthesized Au NPs for catalytic and antimicrobial applications. *J. King Saud Univ. Sci.* **2022**, *34*, 102022.

53. Narayanan KB, Park HH, Han SS. Synthesis and Characterization of Biomatrixed Gold Nanoparticles by the Mushroom Flammulina Velutipes and its Heterogeneous Catalytic Potential. *Chemosphere* **2015**, *141*, 169–175.

54. Narayanan KB, Park HH. Homogeneous Catalytic Activity of Gold Nanoparticles Synthesized Using Turnip (*Brassica Rapa* L.) Leaf Extract in the Reductive Degradation of Cationic azo dye. *Korean J. Chem. Eng.* **2015**, *31*, 1273–1277.

55. Zhao PX, Feng XW, Huang DS, Yang GY, Astruc D. Basic Concepts and Recent Advances in Nitrophenol Reduction by Gold and Other Transition Metal Nanoparticles. *Coord. Chem. Rev.* **2015**, *287*, 114–136.

56. Rajan A, Vilas V, Philip DJ. Studies on Catalytic, Antioxidant, Antibacterial and Anticancer Activities of Biogenic Gold Nanoparticles. *J. Mol. Liq.* **2015**, *212*, 331–339.

57. Yan Y, Ma X, Xia Y, Feng H, Liu S, He C, et al. Mechanism of highly efficient electrochemical degradation of antibiotic sulfadiazine using a layer-by-layer GNPs/PbO$_2$ electrode. *Environ. Res.* **2023**, *217*, 114778.